

Modeling the Shape of the Brain Connectome via Deep Neural Networks

Haocheng Dai , Martin Bauer , P. Thomas Fletcher , Sarang C. Joshi 

 University of Utah

 Florida State University

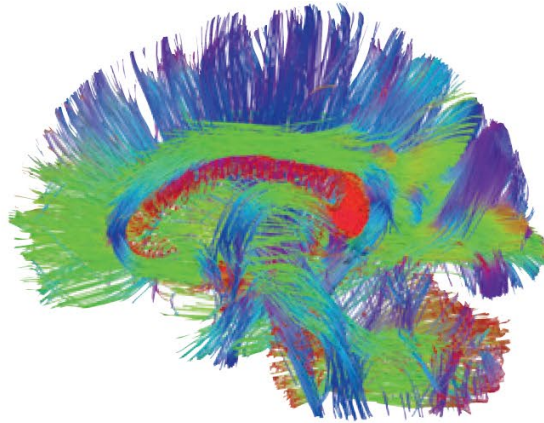
 University of Virginia

IPMI 2023

What is brain connectome?

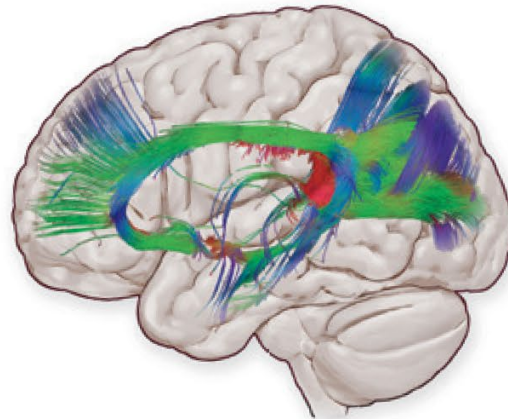
A comprehensive map of neuronal connections

A Map of Anatomical Connectivity

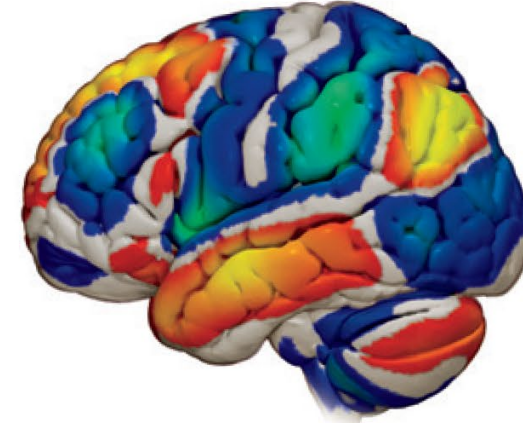


Tractography

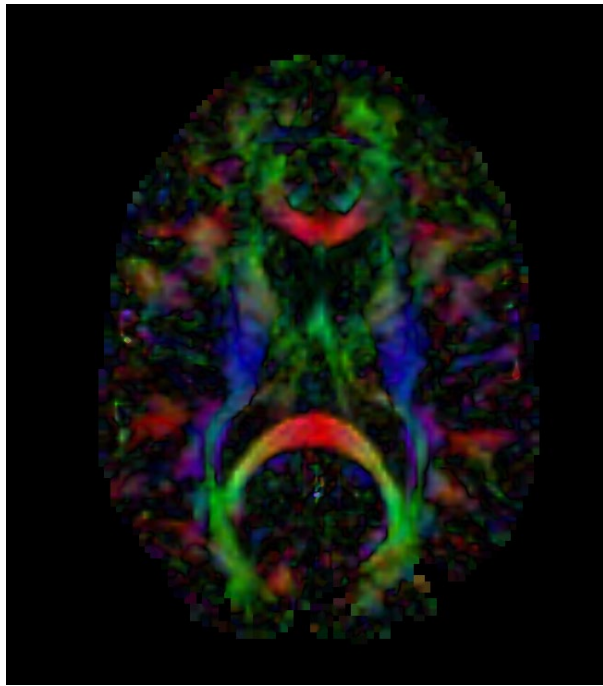
B Specific Fiber Tracts



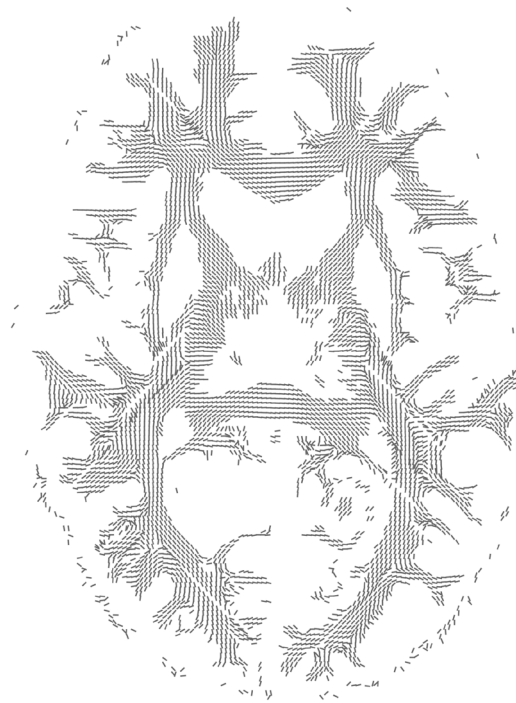
C Map of Functional Connectivity



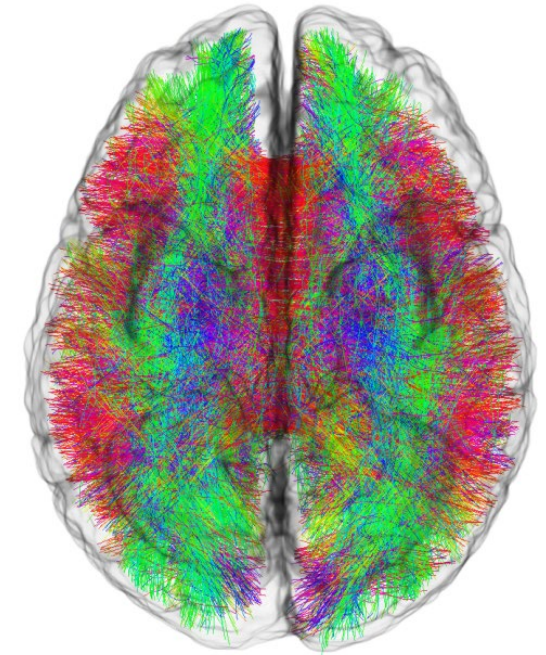
How do we infer tractography?



Diffusion MRI



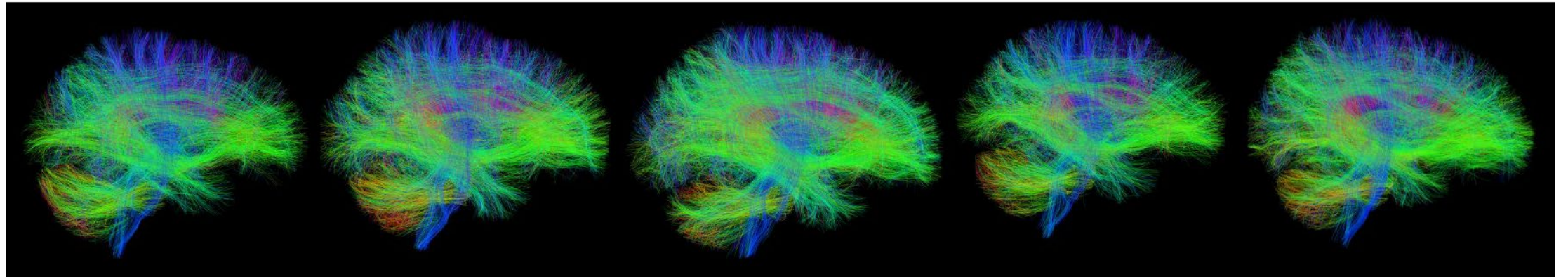
Vector Field



Tractography



How do we statistically analyze a population of connectomes?

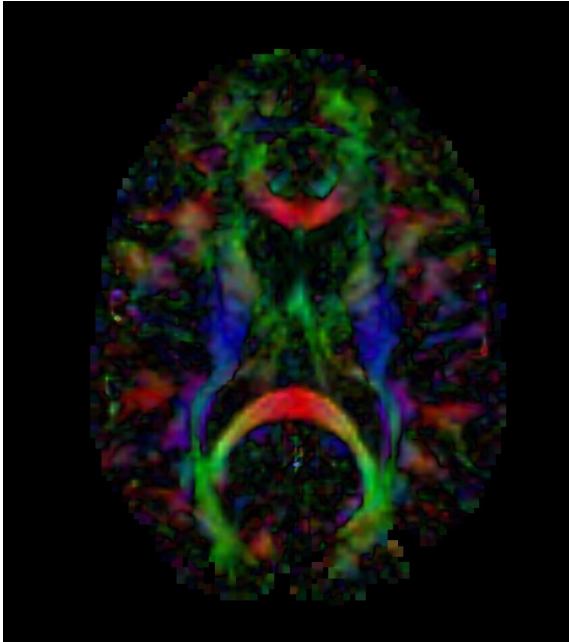


Construct connectome **Riemannian manifold** atlas from tractography data to statistically quantify the geometric variability of structural connectivity across a population.

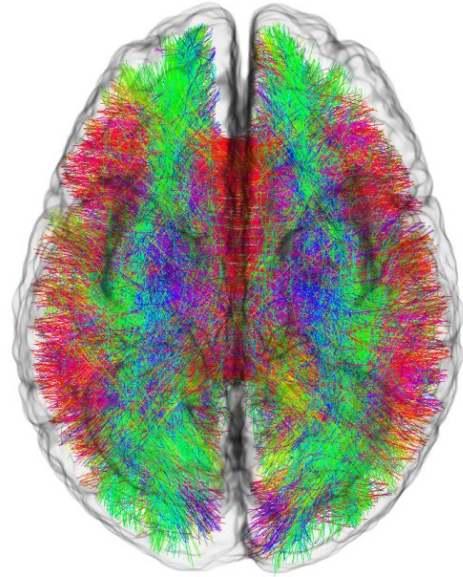


Geodesic Tractography

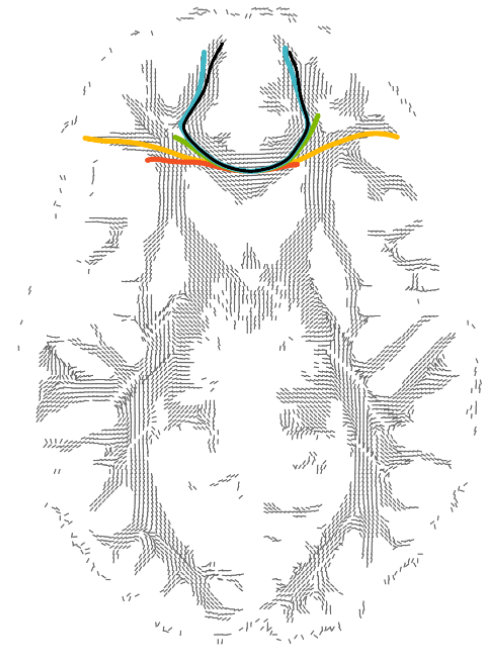
— Tractography — Geodesic



Diffusion MRI

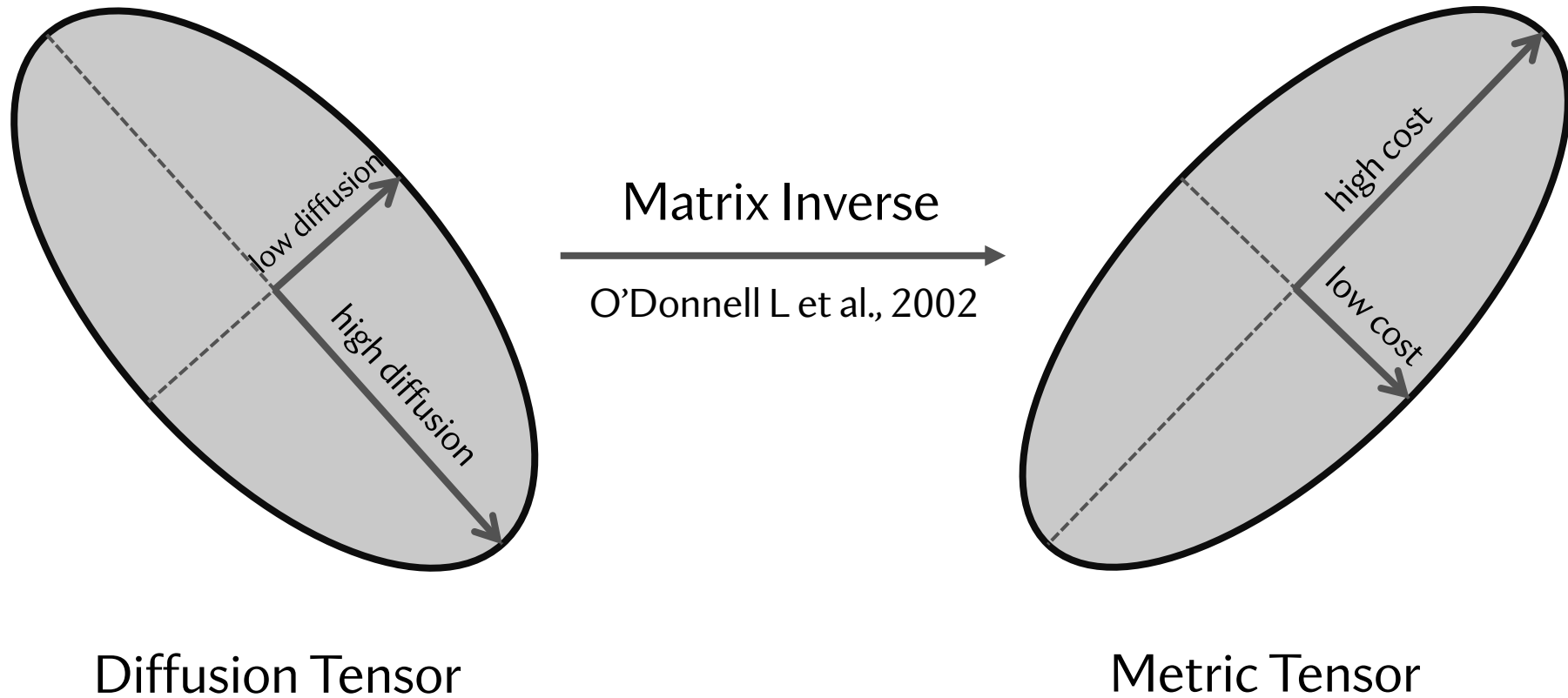


Tractography

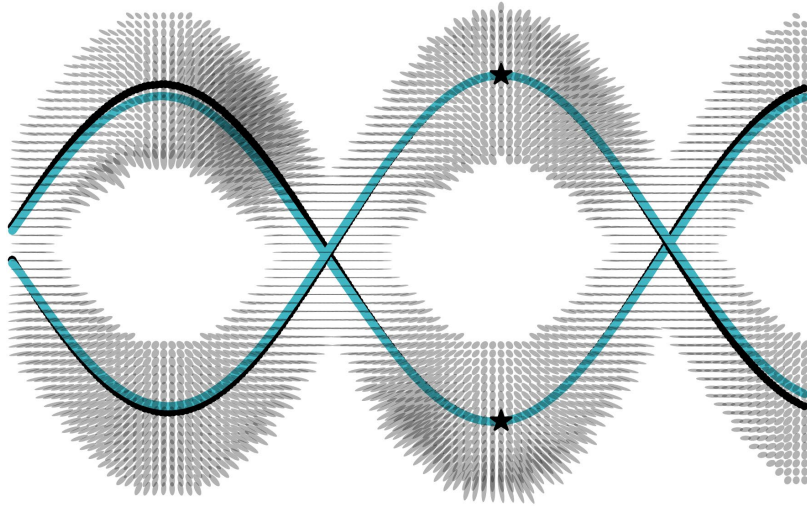


Riemannian Manifold

Related Work

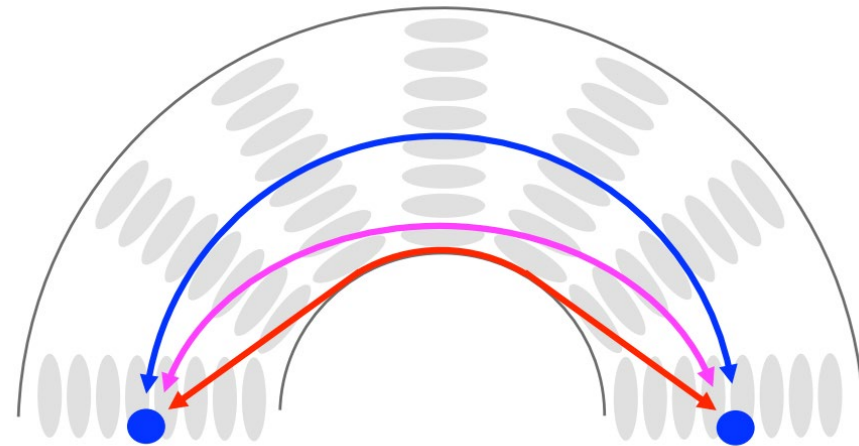


Pros and Cons of Geodesic Tractography



Advantage of geodesic tractography

- Can find tracts between two endpoints;
- A tool of studying geometry of the brain.



Disadvantage of previous geodesic tractography

- Easy deviation in high-curvature area (does not take neighbor metric variation into consideration);
- Unable to characterize crossing fibers

Hao et al., 2011

What is a metric tensor?

Metric tensor defines how we calculate the inner product under a given space.

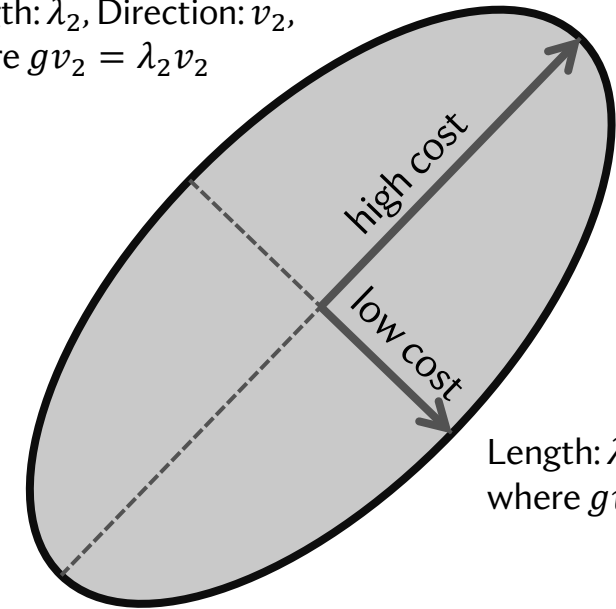
$$g(u, v) = u^T g v,$$
$$g(v, v) = \|v\|^2 = v^T g v,$$

where $g \in \mathbb{R}^{n \times n}$, n is the dimension of the space.

Euclidean metric	$g = I$
Riemannian metric	g can be any SPD matrix

Visualization of metric tensor

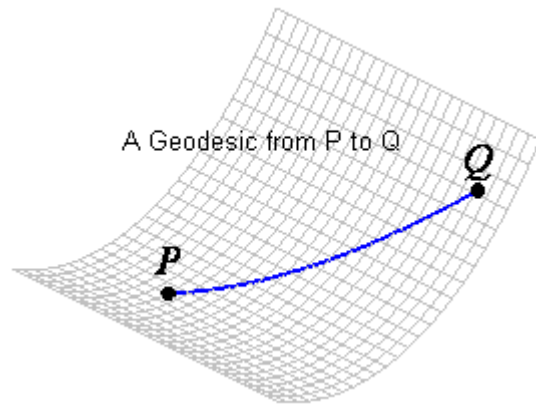
Length: λ_2 , Direction: v_2 ,
where $g v_2 = \lambda_2 v_2$



Length: λ_1 , Direction: v_1 ,
where $g v_1 = \lambda_1 v_1$

The axis of the ellipsoid is regulated by the eigenvector and eigenvalue of the metric tensor.

What is a geodesic?



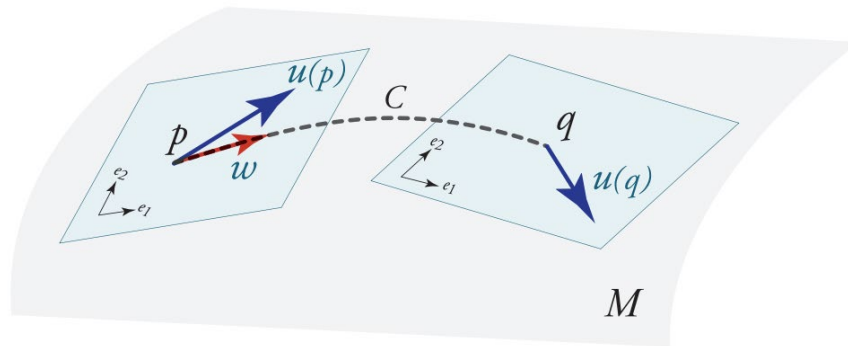
The speed of a geodesic on a Riemannian manifold is constant, i.e. the tangential acceleration of a geodesic is zero.

To compute geodesic curves, we need to find curves where the acceleration vector is normal to the space, namely

$$\nabla_{\dot{\gamma}} \dot{\gamma} = 0$$

holds along the curve γ , where ∇ is called covariant derivative, or Levi-Civita connection.

What is covariant derivative?



Intuitively, covariant derivative

$$\nabla_w u$$

is a rate of change vector at u of a vector field in the direction of w , taking changes of the coordinate system into account.

Covariant derivative is the generalization of the directional derivative. It provides a connection between tangent spaces in a curved space.

Estimating Riemannian Metrics from Geodesics

Explicitly, covariant derivative $\nabla_{\mathcal{V}}^g \mathcal{V}$ can be written as

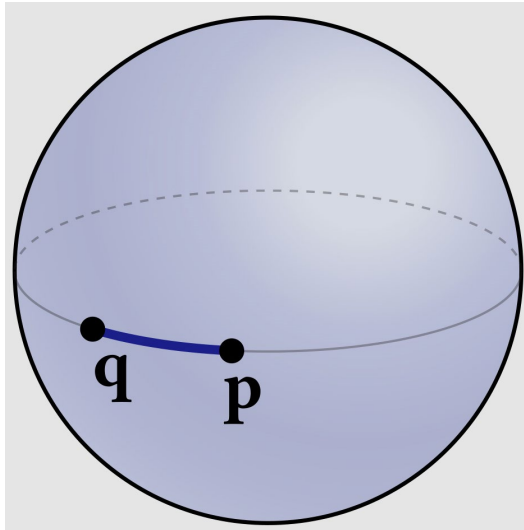
$$\nabla_{\mathcal{V}}^g \mathcal{V} = \sum_k \left(\sum_i v^i \frac{\partial v^k}{\partial x^i} + \sum_{i,j} \Gamma_{ij}^k v^i v^j \right) e_k. \quad (4)$$

A vector field \mathcal{V} is called a geodesic vector field if and only if it satisfies the equations

$$\begin{aligned} \nabla_{\mathcal{V}}^g \mathcal{V} &= 0, \text{ (unit)} \\ \nabla_{\mathcal{V}}^g \mathcal{V} &= \sigma \mathcal{V}, \text{ (non-unit)} \end{aligned}$$

where $\mathcal{V} = v^i e_i$ with $e_i = \frac{\partial}{\partial x^i}$ being the i -th basis vector, and $\sigma = \frac{\nabla_{\mathcal{V}} \mathcal{V}^T \mathcal{V}}{\mathcal{V}^T \mathcal{V}}$.

How is geodesic related to Riemannian metric?



As shown by Spivak, a critical curve for

$$L(\gamma) = \int_0^1 \frac{1}{2} \|\dot{\gamma}(t)\|^2 dt \quad (1)$$

is also a critical curve for

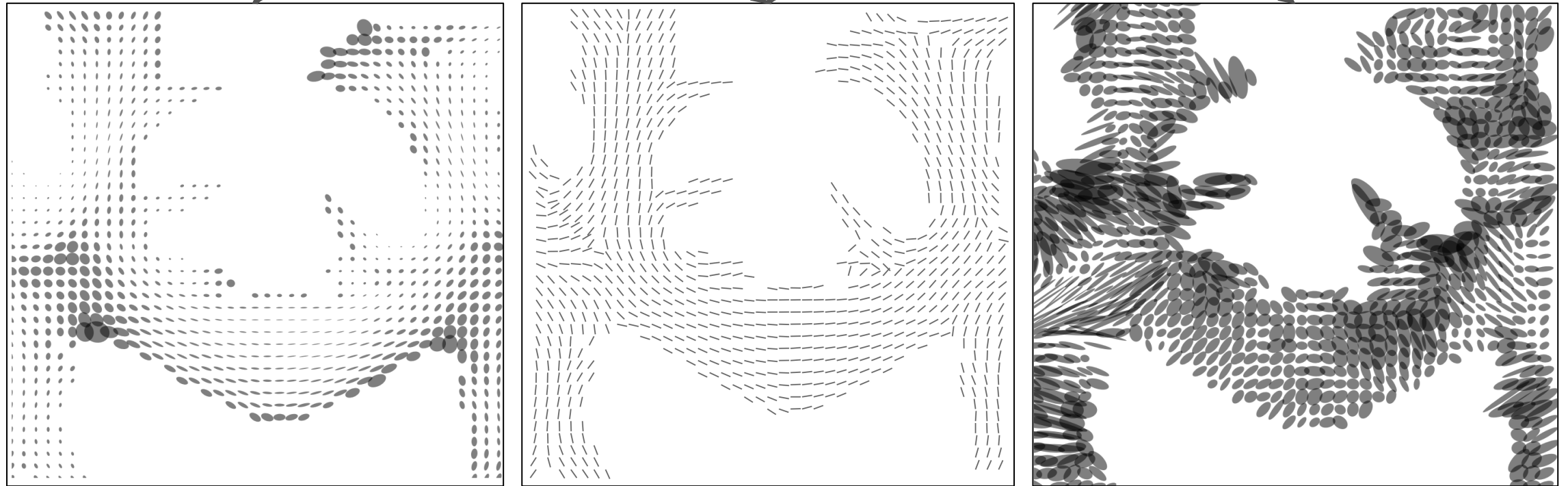
$$L(\gamma) = \int_0^1 \|\dot{\gamma}(t)\| dt. \quad (2)$$

The only difference is that the geodesic that minimizes (1) has a constant speed.

Estimating Riemannian Metrics from Geodesics

SOTA tractography method

Metric Estimation via
Neural Network



A. DWMRI

B. Tangent Vector of Tractography

C. Riemannian Metric Field

Estimating Riemannian Metrics from Geodesics

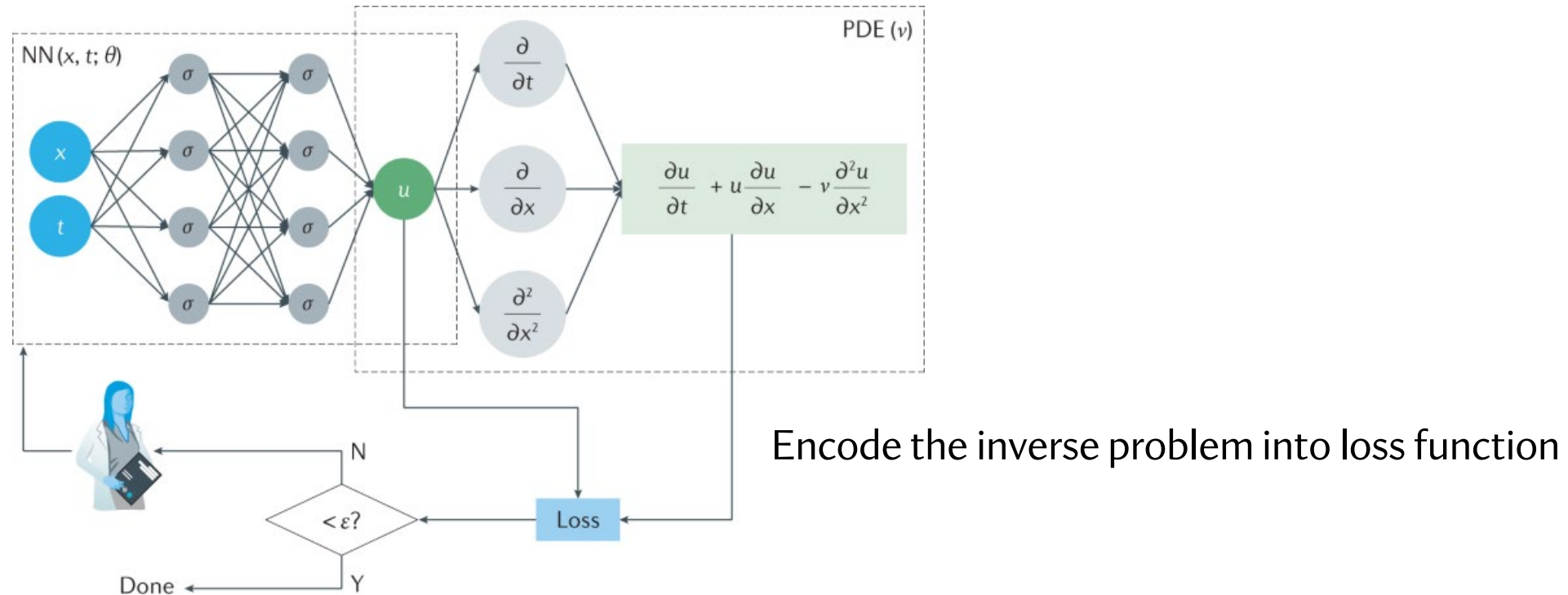
Objective function: Given vector fields $\mathcal{V}_i \in \mathfrak{X}(M), i \in \{1, \dots, m\}$ find the Riemannian metric g on M that minimizes the energy functional

$$E(g) = \sum_i^m \left\| \nabla_{\mathcal{V}_i}^g \mathcal{V}_i - \sigma_i \mathcal{V}_i \right\| + \alpha \cdot \text{Reg}(g),$$

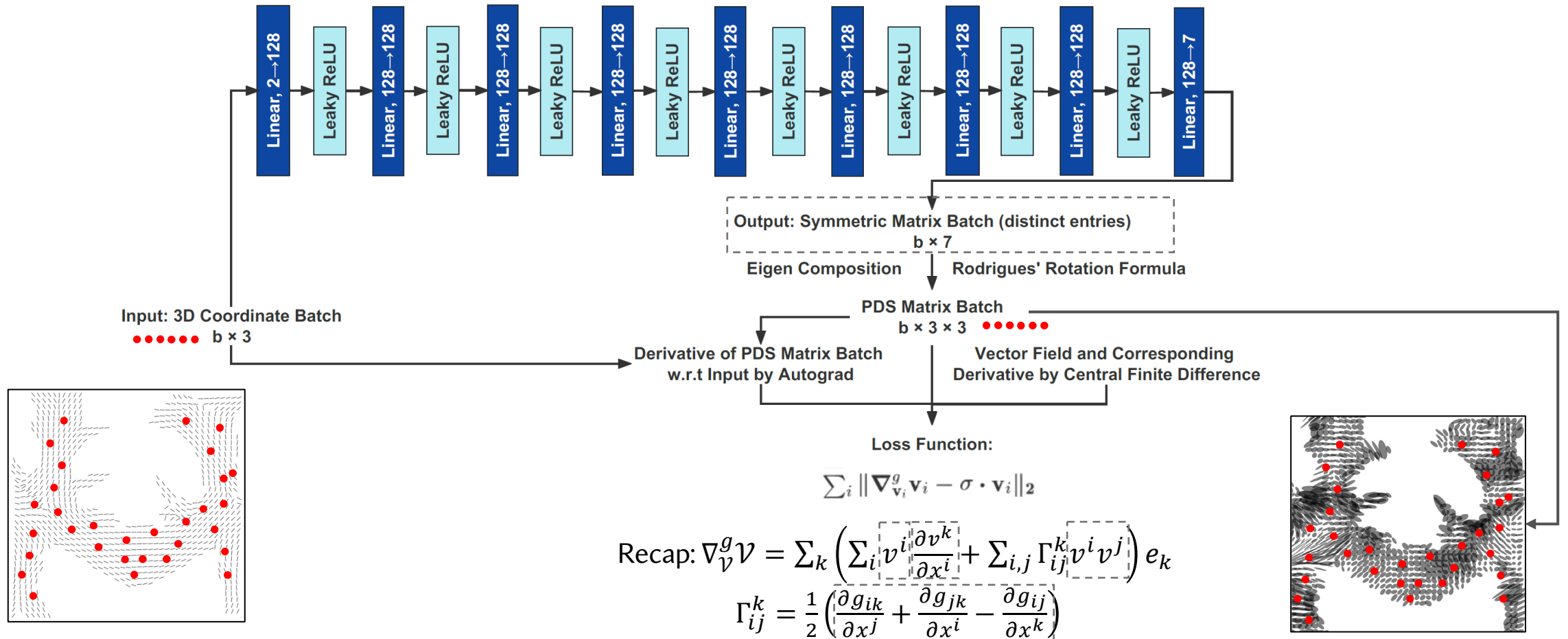
where $\sigma_i = \frac{\nabla_{\mathcal{V}_i} \mathcal{V}_i^T \mathcal{V}_i}{\mathcal{V}_i^T \mathcal{V}_i}$.

Physics-Informed Neural Networks (PINNs)

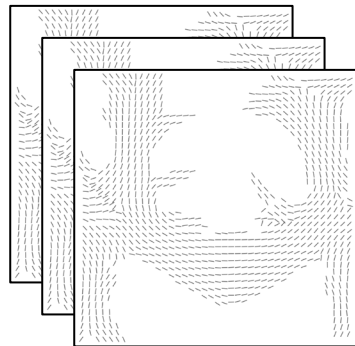
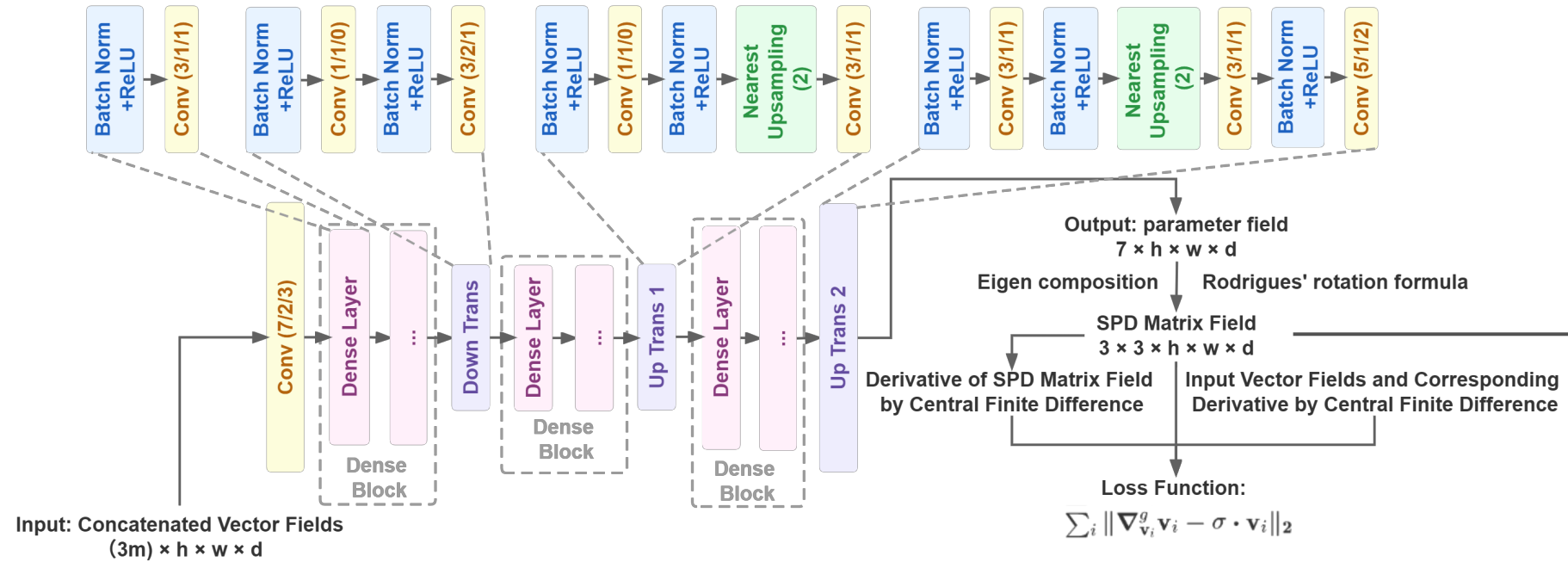
Leverage AutoGrad in PyTorch or TensorFlow to calculate derivative



Architecture: Baseline MLP



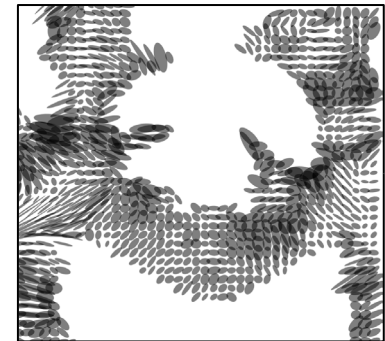
Architecture: CEDNN



Multiple vector fields describe crossing fibers.

*2D example only for illustration purpose.

One metric field accommodates multiple crossing fibers.



SPD Metric Matrix Composition

Matrix Exponential

$$e^S = \sum_{k=0}^{\infty} \frac{1}{k!} S^k$$

$$S = \begin{bmatrix} u_1 & u_2 & u_3 \\ u_2 & u_4 & u_5 \\ u_3 & u_5 & u_6 \end{bmatrix}$$

*In implementation, eigen composition is 5 times faster than matrix exponential.

Eigen Composition

Orthogonal \swarrow

$$g = R \Lambda R^T$$

\uparrow
Positive eigenvalues

We formulate orthogonal matrix through Rodrigues rotation formula:

$$R = I + \sin(\theta) K + \cos(\theta) K^2$$

$$I = \begin{bmatrix} 1 & 0 & 0 \\ 0 & 1 & 0 \\ 0 & 0 & 1 \end{bmatrix}, \quad K = \begin{bmatrix} 0 & -u_1 & u_2 \\ u_1 & 0 & -u_3 \\ -u_2 & u_3 & 0 \end{bmatrix},$$

$$\theta = u_4, \quad \Lambda = \begin{bmatrix} \exp(u_5) & 0 & 0 \\ 0 & \exp(u_6) & 0 \\ 0 & 0 & \exp(u_7) \end{bmatrix}$$

Geodesic Shooting

Algorithm 1 Geodesic Shooting

Require: Vector field $\mathbf{v} : M \rightarrow \mathbb{R}^n$; Christoffel symbol $\Gamma_{ij}^k : M \rightarrow \mathbb{R}$ based on metric $g : M \rightarrow \mathbb{R}^{n \times n}$;

starting point $\gamma(\frac{0}{T}) \in M$; proper step size ϵ, η .

$$\dot{\gamma}(\frac{0}{T}) = \mathbf{v}(\gamma(\frac{0}{T}))$$

▷ Linearly interpolate \mathbf{v}

$$\gamma(\frac{1}{T}) = \gamma(\frac{0}{T}) + \epsilon \cdot \dot{\gamma}(\frac{0}{T})$$

for $t = 2 : T$ **do**

$$\ddot{\gamma}^k(\frac{t-2}{T}) = -\Gamma_{ij}^k(\gamma(\frac{t-2}{T})) \cdot \dot{\gamma}^i(\frac{t-2}{T}) \cdot \dot{\gamma}^j(\frac{t-2}{T}) + \sigma \cdot \dot{\gamma}^k(\frac{t-2}{T})$$

▷ Linearly interpolate Γ_{ij}^k

$$\dot{\gamma}(\frac{t-1}{T}) = \dot{\gamma}(\frac{t-2}{T}) + \eta \cdot \ddot{\gamma}(\frac{t-2}{T})$$

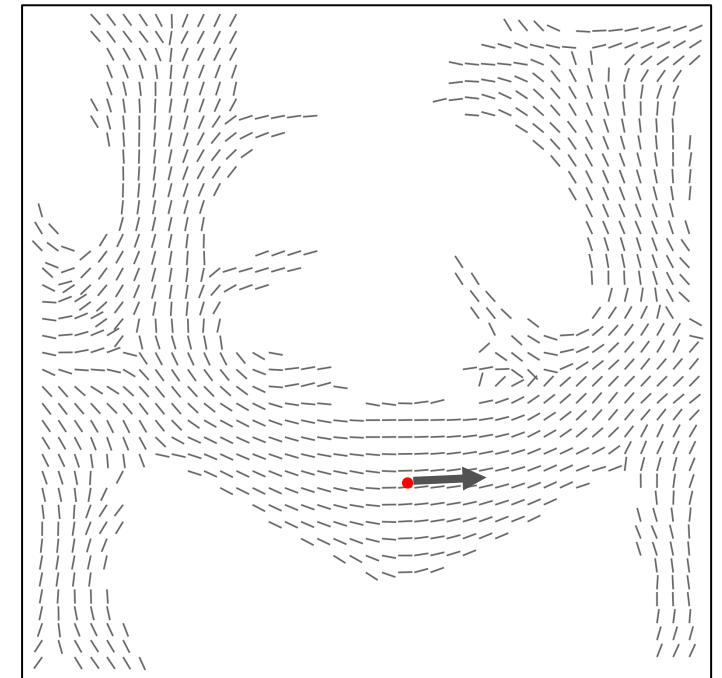
$$\gamma(\frac{t}{T}) = \gamma(\frac{t-1}{T}) + \epsilon \cdot \dot{\gamma}(\frac{t-1}{T})$$

end for

return γ

Geodesic equation (non-unit) recap: $\ddot{\gamma}^k + \Gamma_{ij}^k \dot{\gamma}^i \dot{\gamma}^j = \sigma \cdot \dot{\gamma}^k$

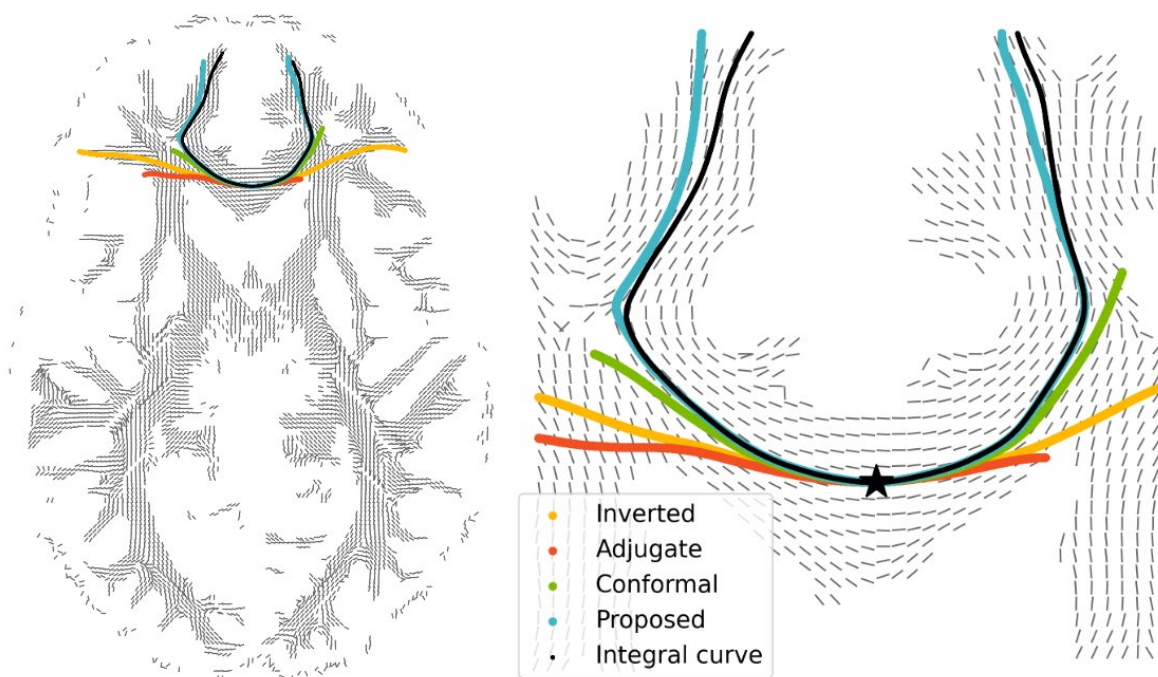
Christoffel symbol recap: $\Gamma_{ij}^k = \frac{1}{2} \left(\frac{\partial g_{ik}}{\partial x^j} + \frac{\partial g_{jk}}{\partial x^i} - \frac{\partial g_{ij}}{\partial x^k} \right)$



- Starting point: $\gamma(0)$
- Initial shooting direction: $\mathcal{V}(\gamma(0))$

Experiment 1: 2D Brain Slices

Inverted	O'Donnell et al., 2002	Take the inverse of the diffusion tensor as metric
Adjugate	Fuster et al., 2016	Take the adjugate of the diffusion tensor as metric
Conformal	Hao et al., 2011	Apply scalar field modulation to inverted diffusion tensor



38 HCP brain subjects, 400 seed points on each subject, 15200 pairs of geodesics and tractography in total

Experiment 1: 2D Brain Slices

Mean min errors:

$$Error(P, Q) = \frac{1}{|P|} \sum_{p \in P} \min_{q \in Q} \|p - q\|_2,$$

where P denotes a tractography and Q our geodesic tractography curve starting at the same seed point.

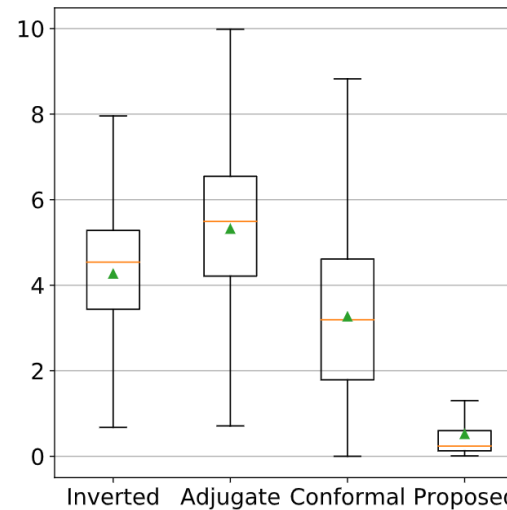
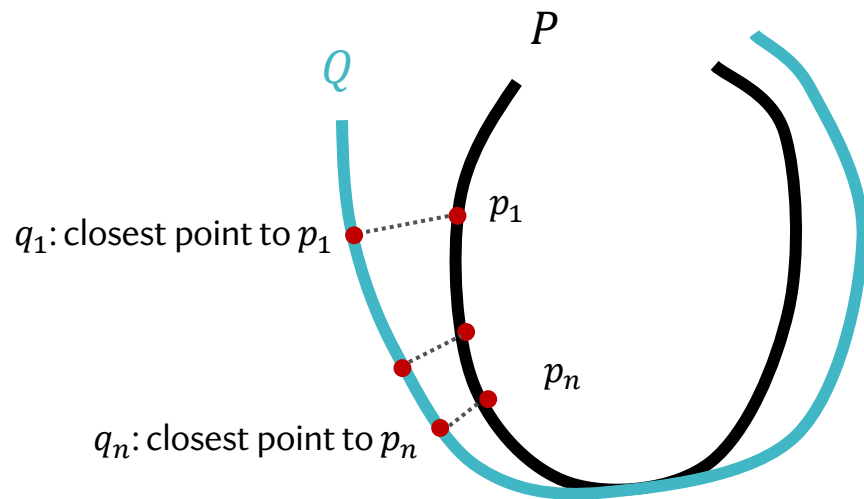


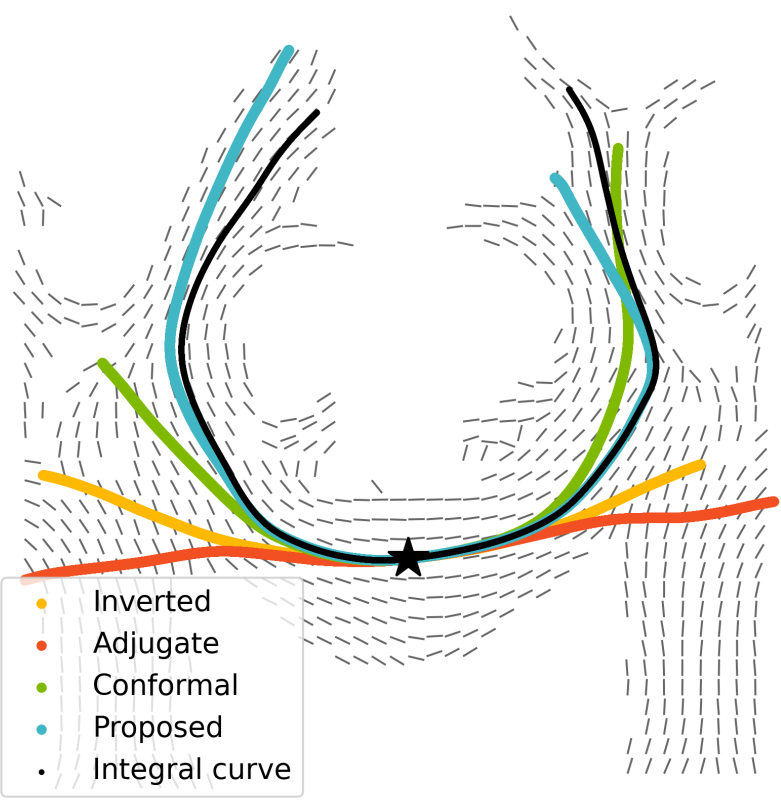
Table 1: Mean and median of mean min errors across different methods over 38 HCP subjects.

Methods	Mean	Median
Inverted	4.2660	4.5393
Adjugate	5.3153	5.4906
Conformal	3.2658	3.1915
Proposed	0.5172	0.2388

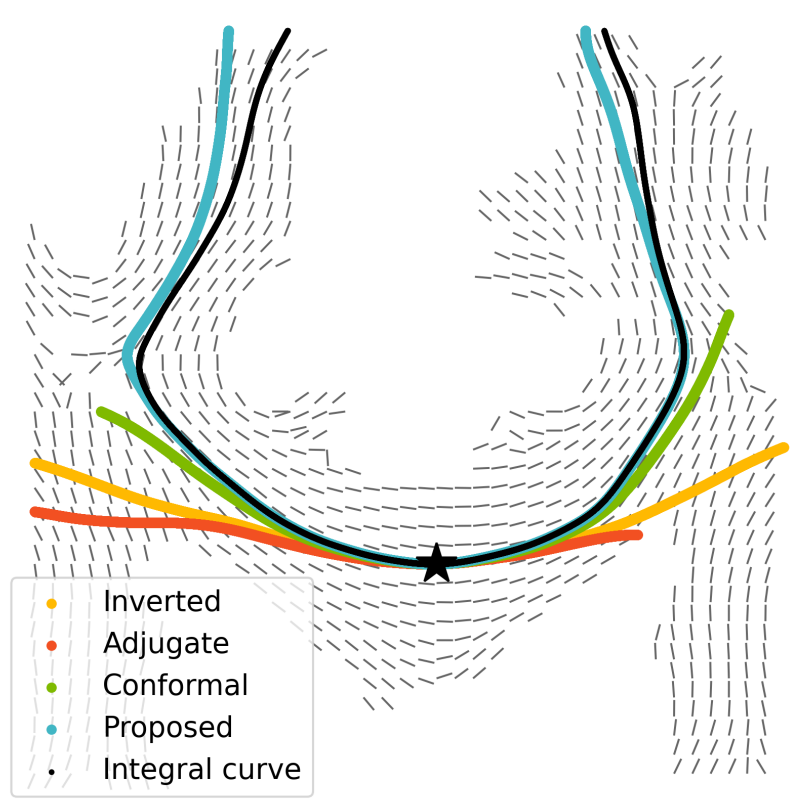
- ▲ mean of the mean min errors distribution
- median of the mean min errors distribution



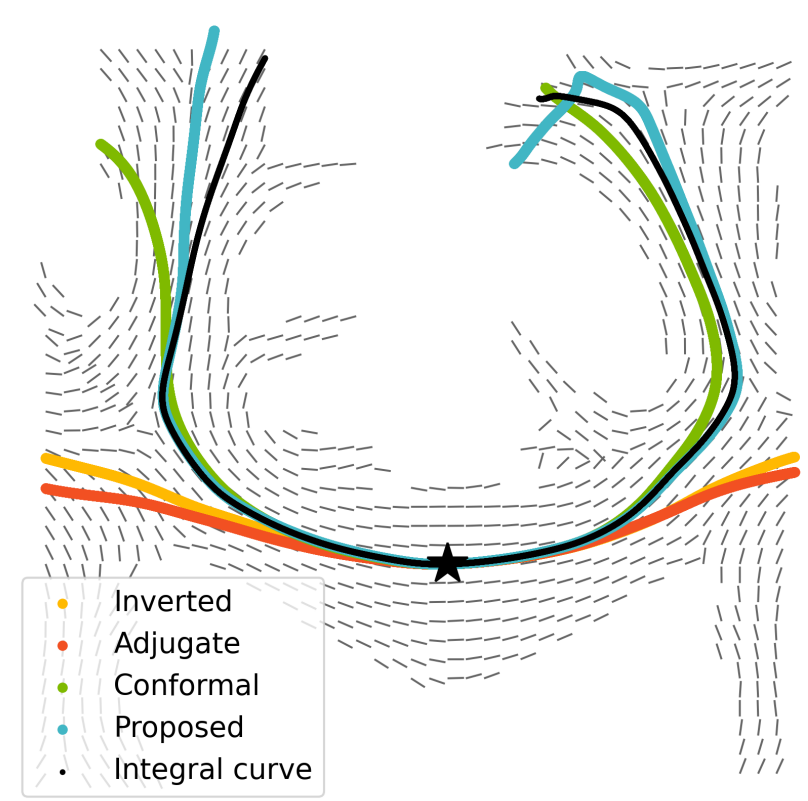
Experiment 1: 2D Brain Slices



101006

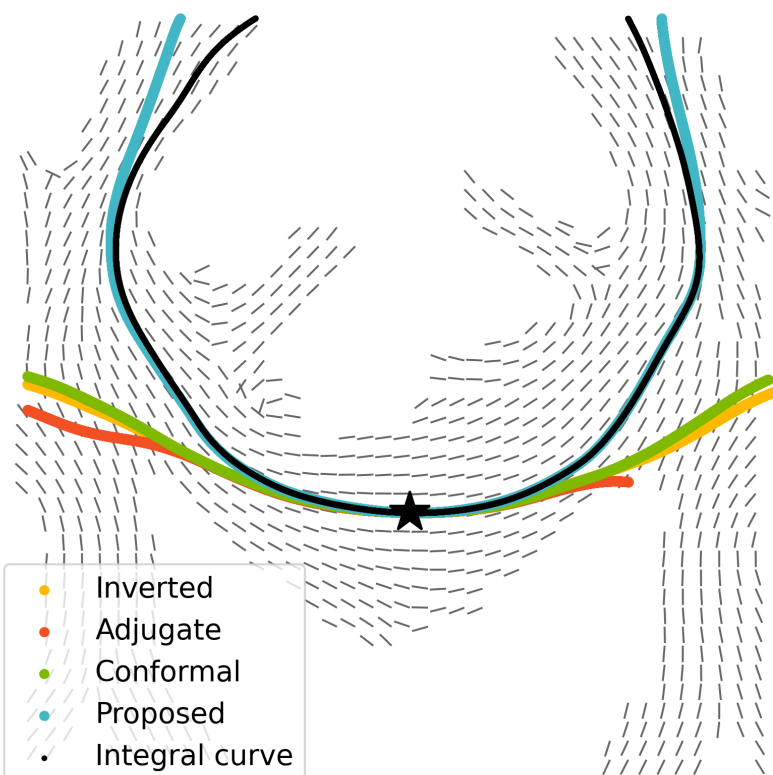


100610

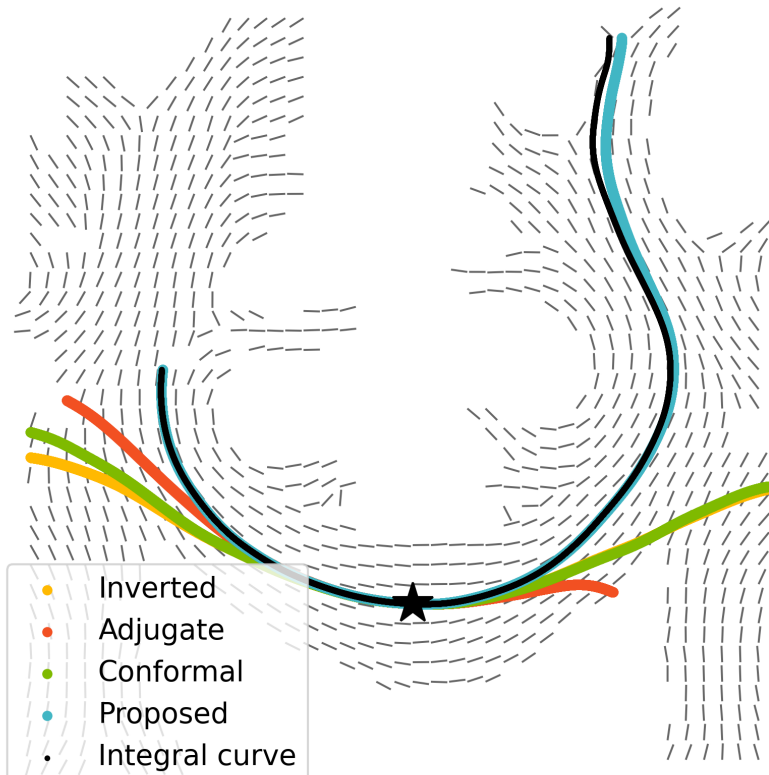


100206

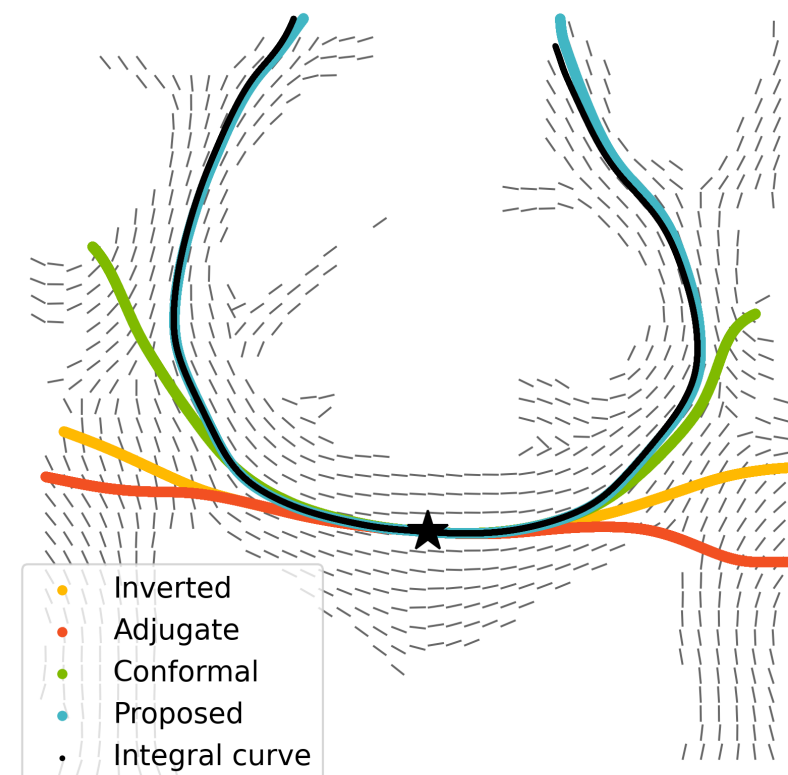
Experiment 1: 2D Brain Slices



102109

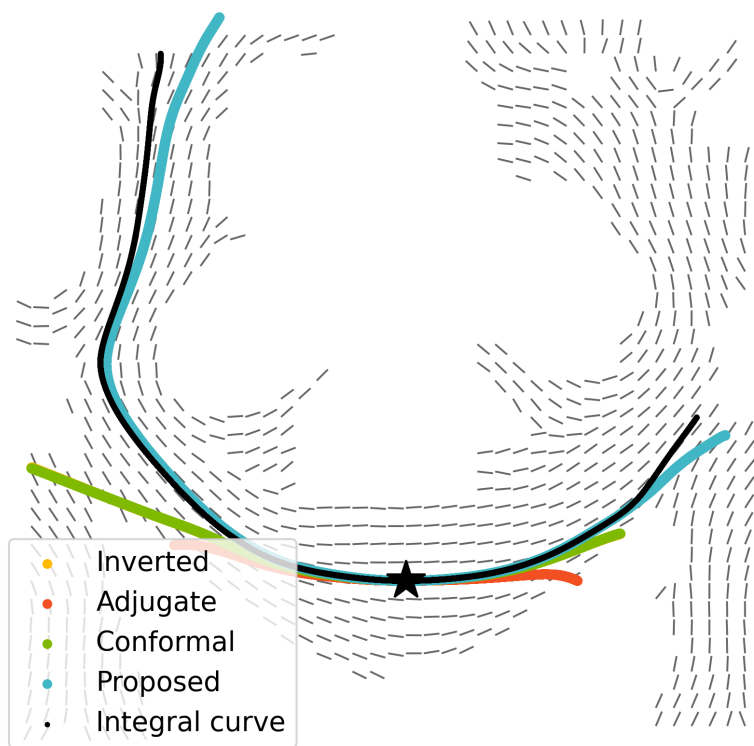


102008

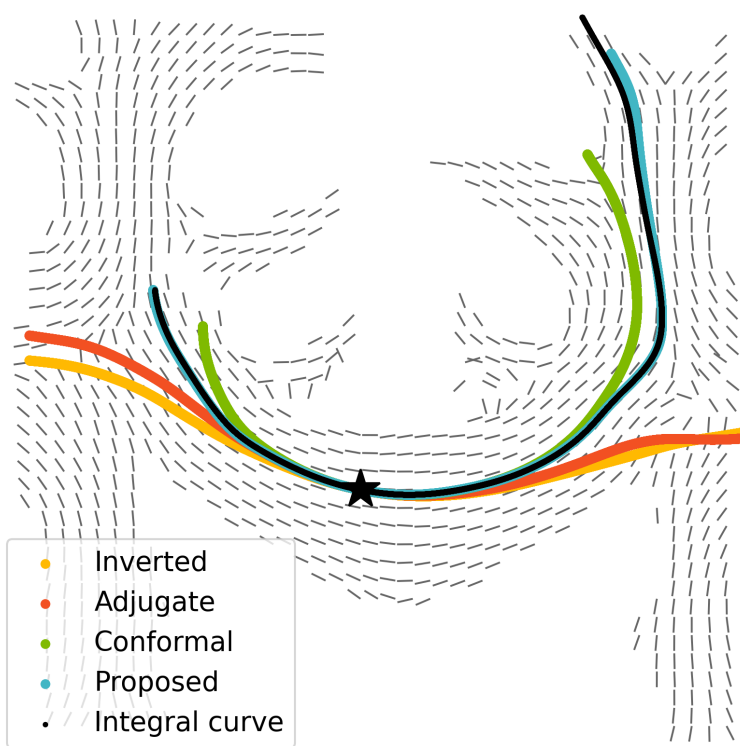


101410

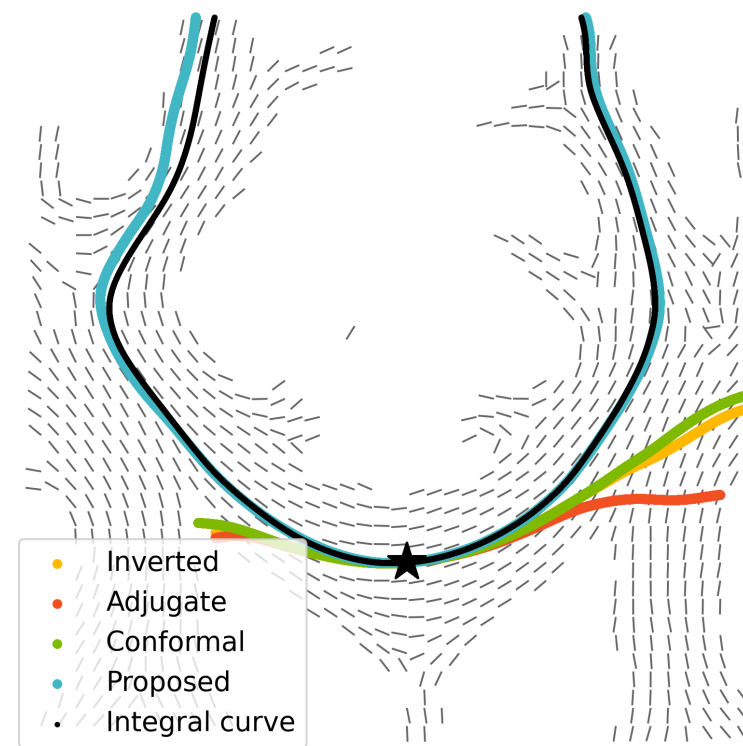
Experiment 1: 2D Brain Slices



102513

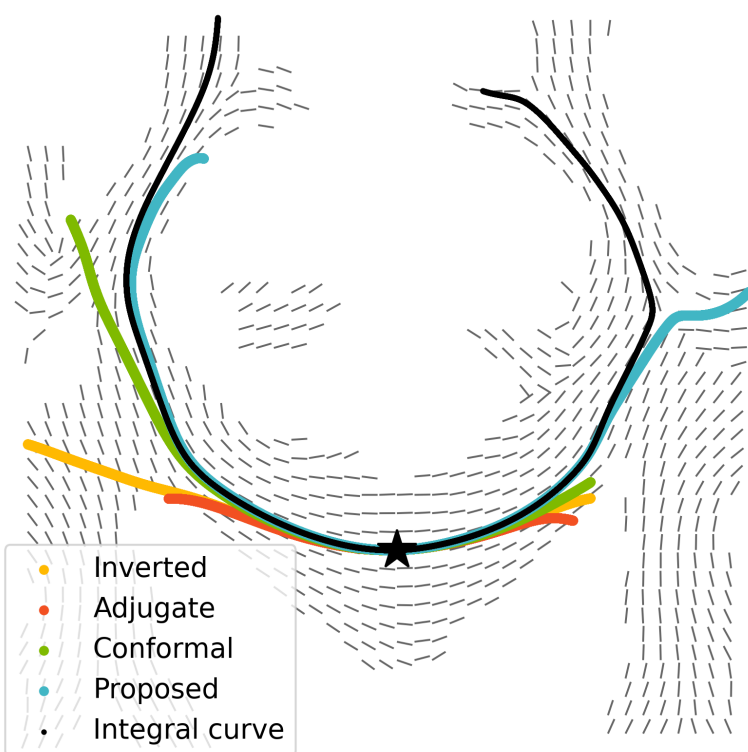


102715

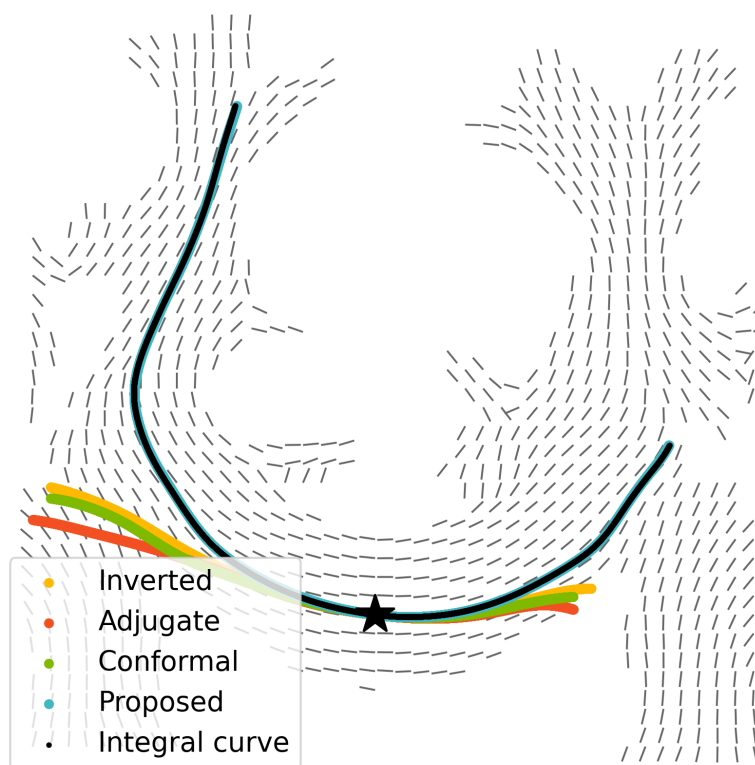


102614

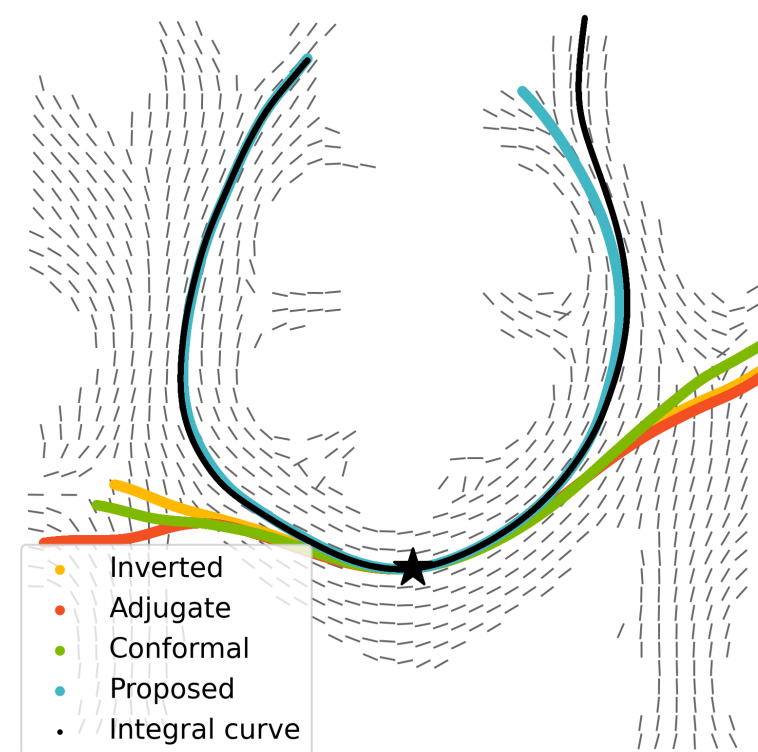
Experiment 1: 2D Brain Slices



103010

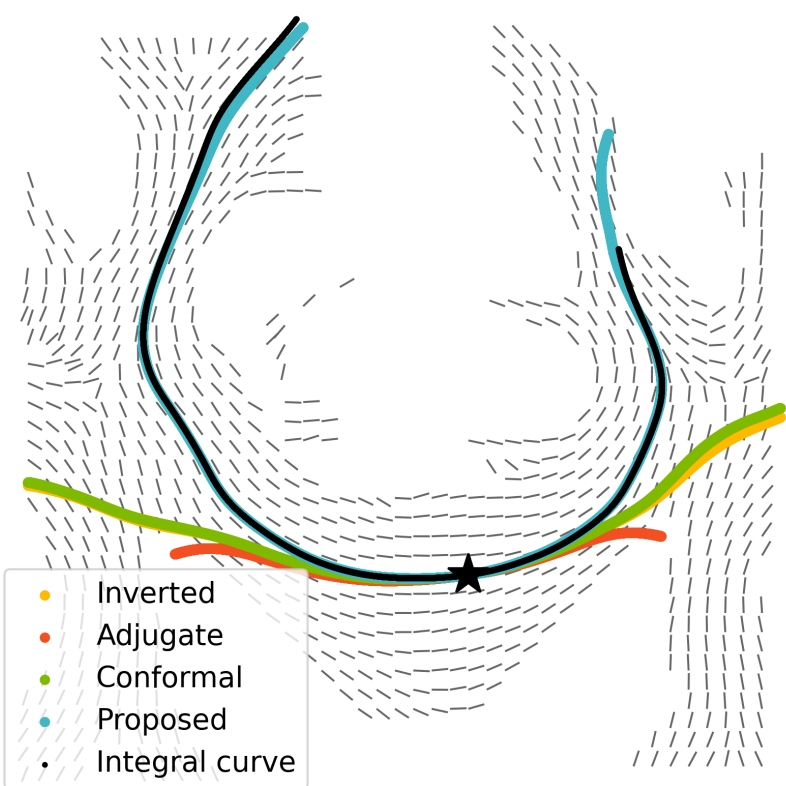


102816

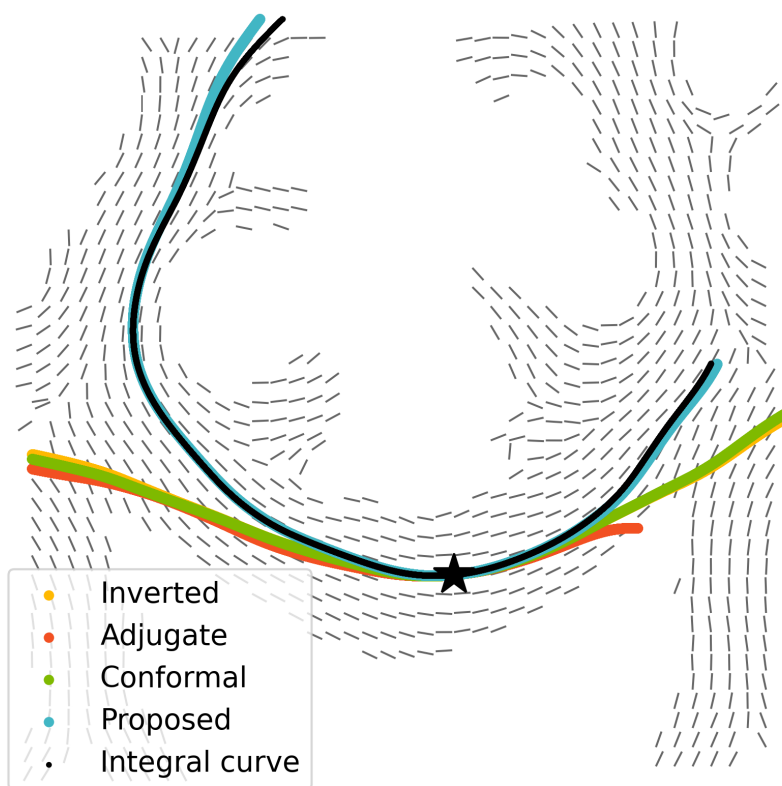


103515

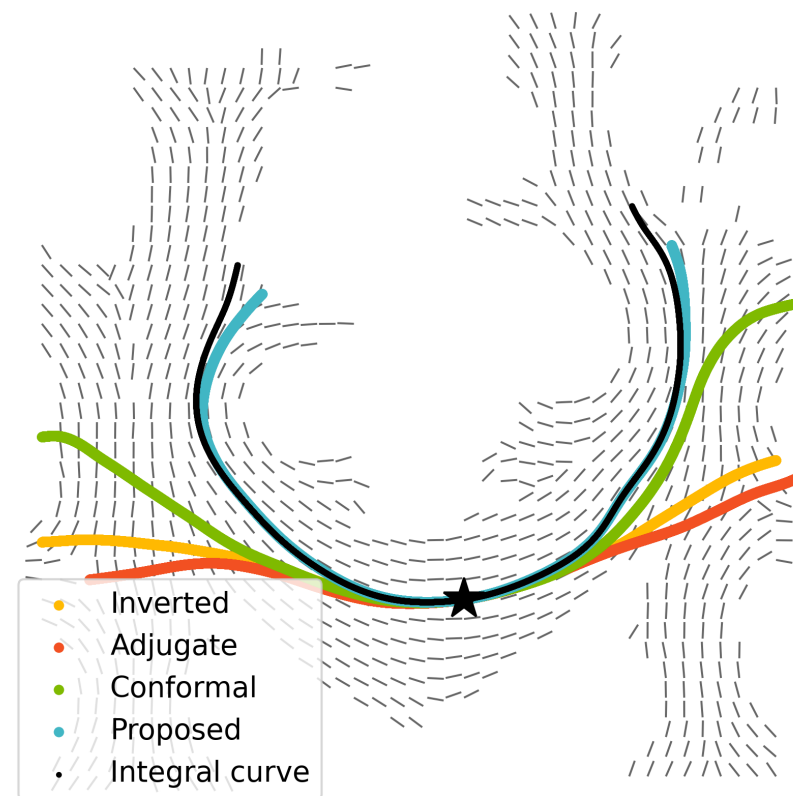
Experiment 1: 2D Brain Slices



104012

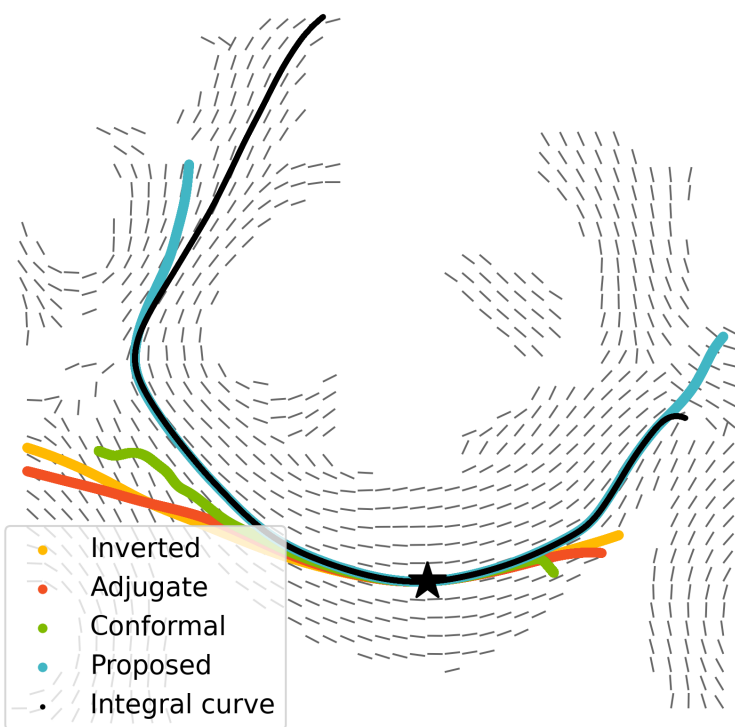


105216

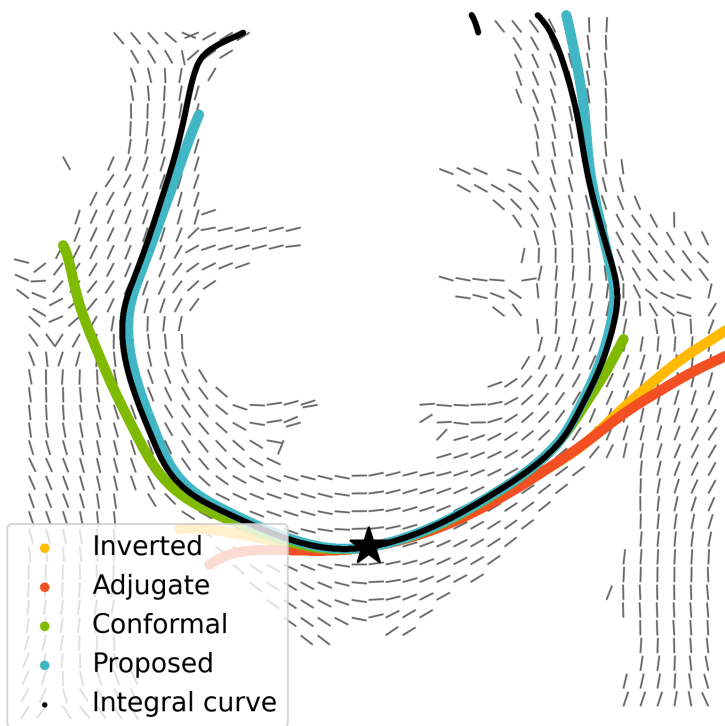


107018

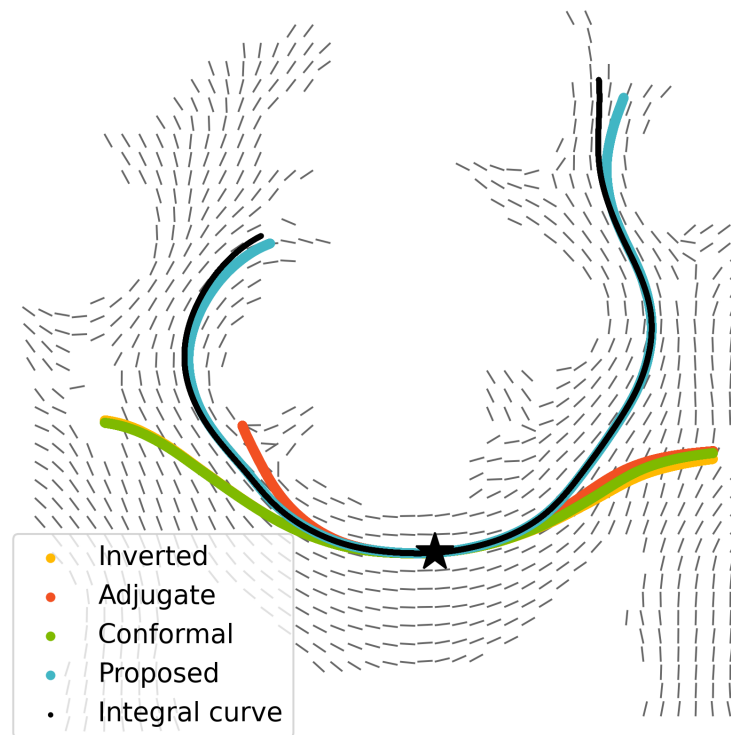
Experiment 1: 2D Brain Slices



108323

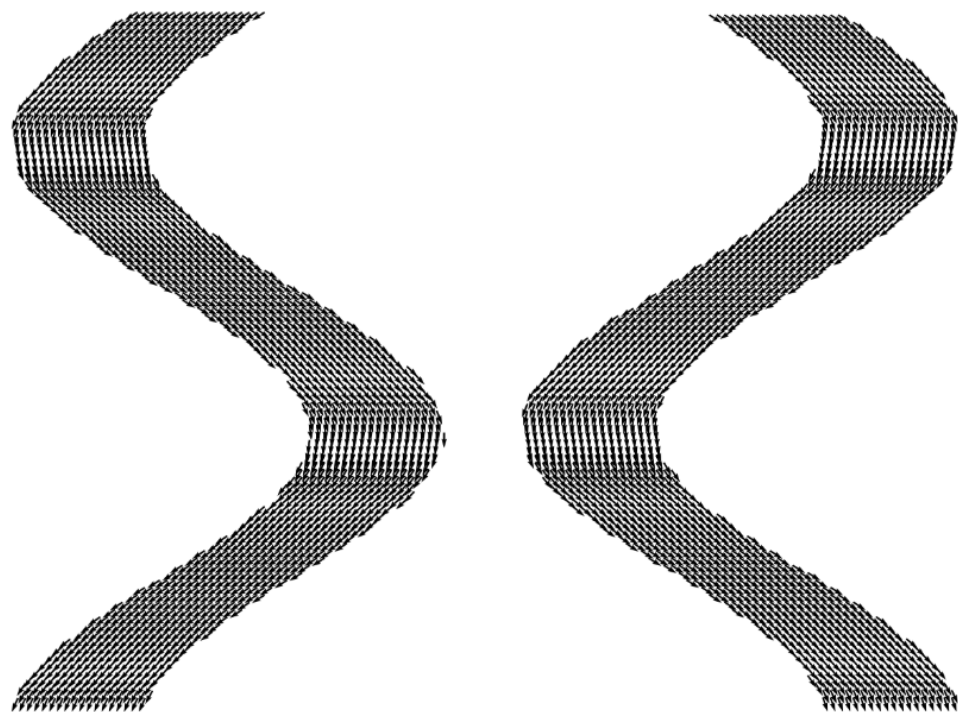


109123



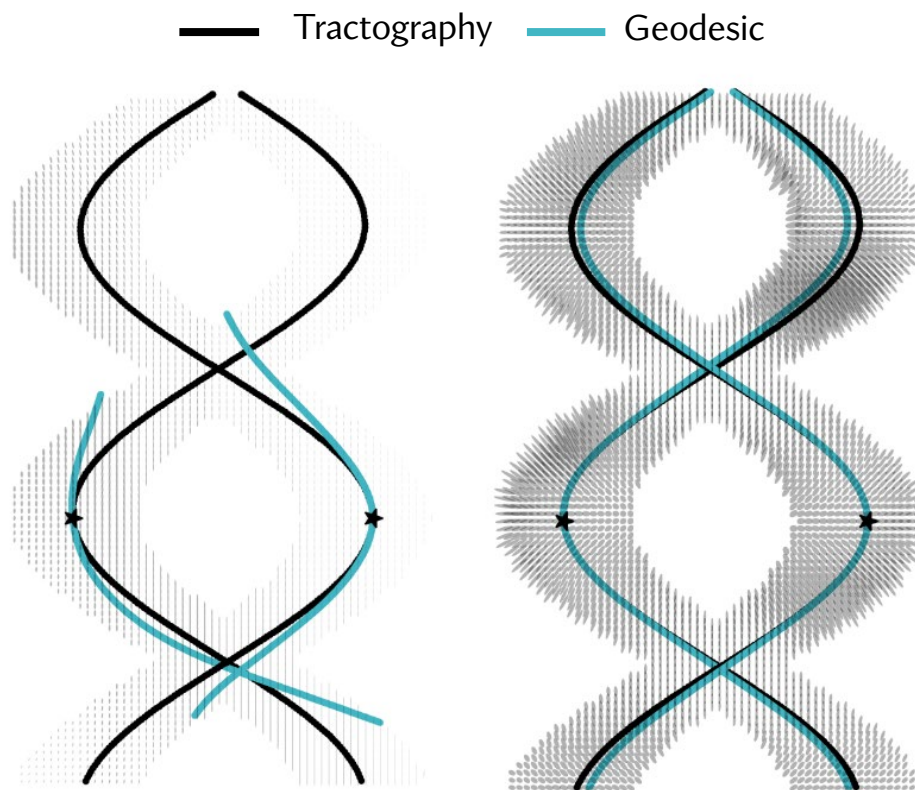
107321

Experiment 2: 2D Synthetic “Braid”



(a) vector field \mathbf{v}_1

(b) vector field \mathbf{v}_2



(c) metric g^P

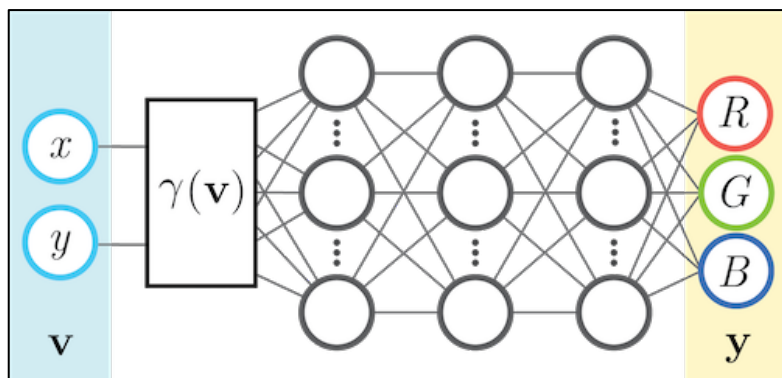
(d) metric g^C

By MLP
(0.7M params)

By CEDNN
(0.7M params)

Experiment 2: 2D Synthetic “Braid”

Fourier feature

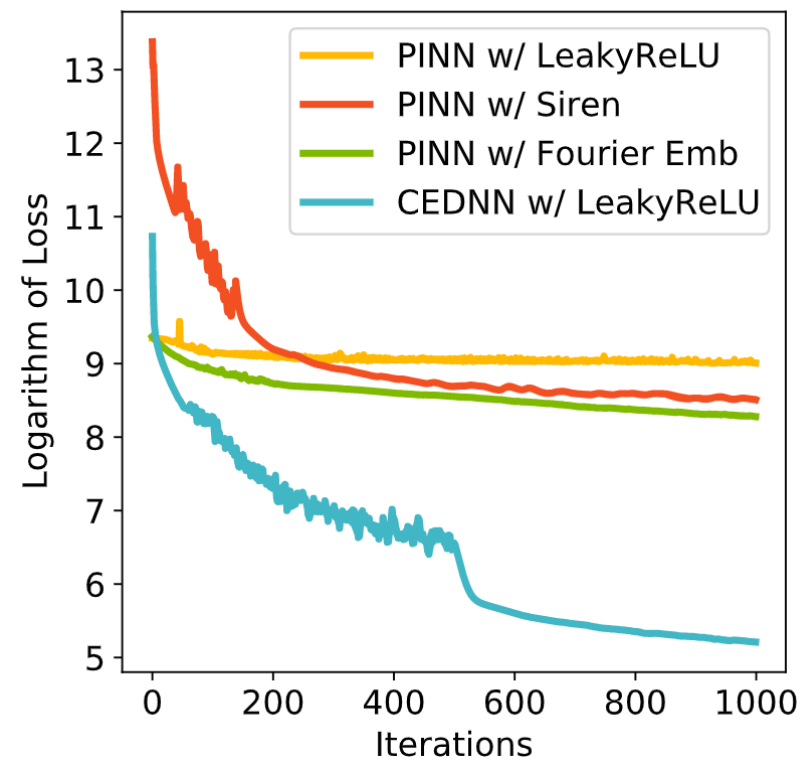


Tancik M et al., 2020

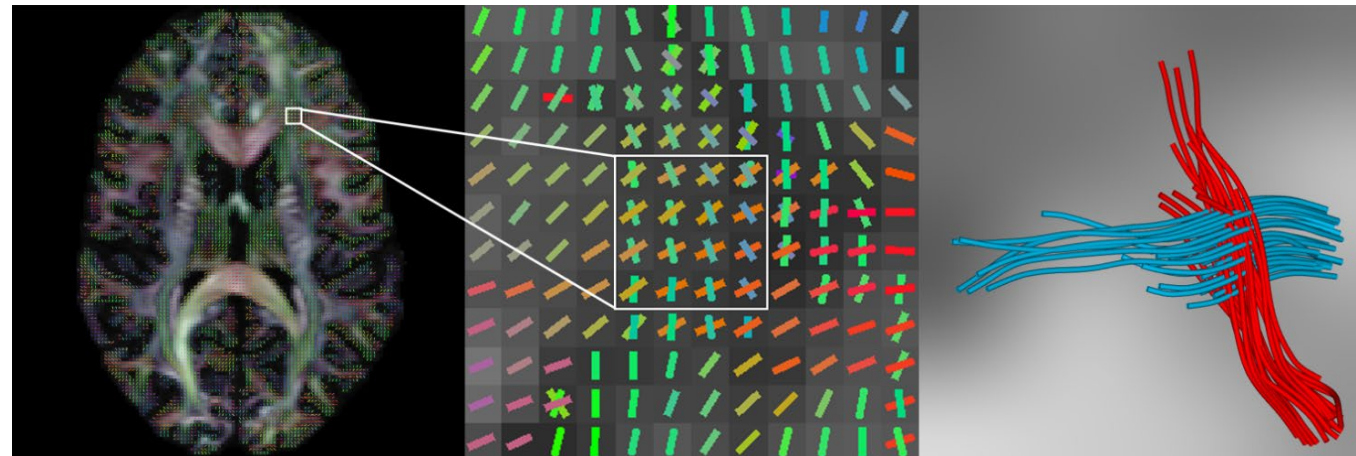
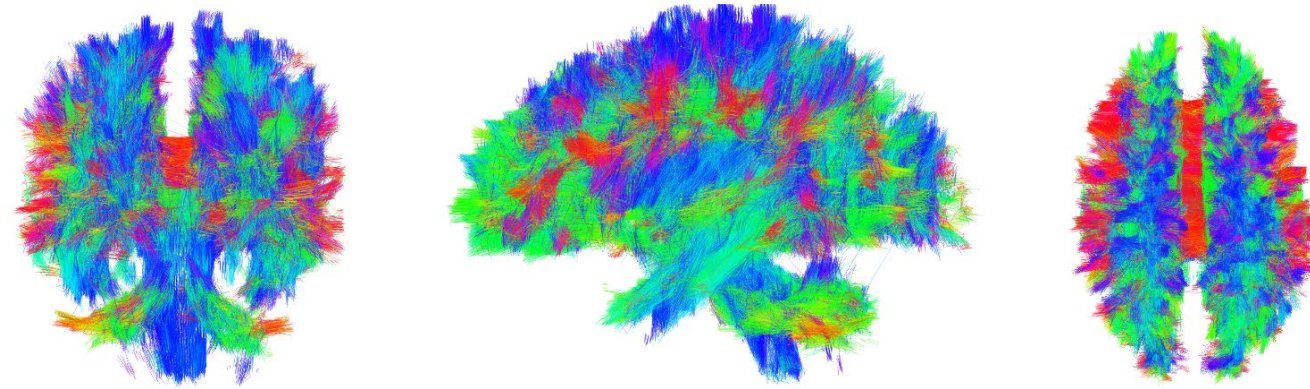
SIREN activation function

$$\mathbf{x}_i \mapsto \phi_i(\mathbf{x}_i) = \sin(\mathbf{W}_i \mathbf{x}_i + \mathbf{b}_i)$$

Sitzmann V et al., 2020



Experiment 3: 3D Brains



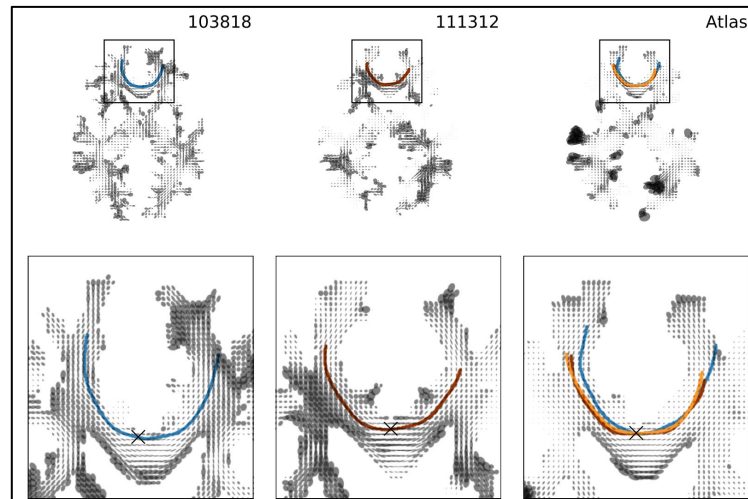
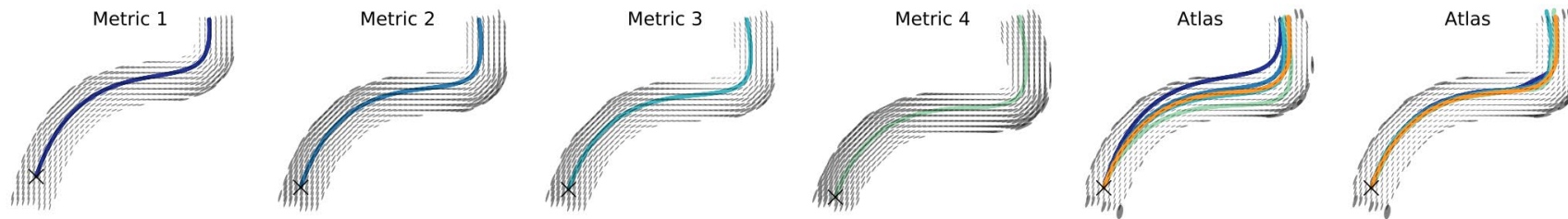


Conclusions

1. We proposed to estimating a Riemannian metric of the brain manifold via deep neural network for the first time.
2. We show that our proposed method outperforms any of the previously proposed methods in geodesic tractography by a large margin.
3. In addition, our approach solves the long-standing issue of these previous methods: the inability to recover crossing fibers with high fidelity.
4. One limitation of the proposed method is that the generalization ability of the trained model to the unseen data is relatively weak.

Future Work

With the ability to robustly and efficiently model the white matter of the brain as a Riemannian manifold, one can directly apply geometrical statistical techniques such as statistical atlas construction, principal geodesic analysis to precisely study the variability and differences in white matter architecture.





Scan the QR code for more project details



Derivation of σ

$$\begin{aligned}\nabla_{\mathbf{v}}^g \frac{\mathbf{v}}{\|\mathbf{v}\|_g} &= \nabla_{\mathbf{v}}^g \mathbf{v} \cdot \frac{1}{\|\mathbf{v}\|_g} + \mathbf{v} \cdot \nabla_{\mathbf{v}}^g \frac{1}{\|\mathbf{v}\|_g} \\ &= \frac{\nabla_{\mathbf{v}}^g \mathbf{v}}{\|\mathbf{v}\|_g} + \mathbf{v} \cdot \nabla_{\mathbf{v}}^g \langle \mathbf{v}, \mathbf{v} \rangle_g^{-\frac{1}{2}} \\ &= \frac{\nabla_{\mathbf{v}}^g \mathbf{v}}{\|\mathbf{v}\|_g} + \mathbf{v} \cdot \left(-\frac{1}{2} \right) \cdot \langle \mathbf{v}, \mathbf{v} \rangle_g^{-\frac{3}{2}} \cdot \nabla_{\mathbf{v}}^g \langle \mathbf{v}, \mathbf{v} \rangle \\ &= \frac{\nabla_{\mathbf{v}}^g \mathbf{v}}{\|\mathbf{v}\|_g} - \frac{1}{2} \mathbf{v} \cdot \langle \mathbf{v}, \mathbf{v} \rangle_g^{-\frac{3}{2}} \cdot (\langle \nabla_{\mathbf{v}}^g \mathbf{v}, \mathbf{v} \rangle_g + \langle \mathbf{v}, \nabla_{\mathbf{v}}^g \mathbf{v} \rangle_g) \\ &= \frac{\nabla_{\mathbf{v}}^g \mathbf{v}}{\|\mathbf{v}\|_g} - \mathbf{v} \cdot \langle \mathbf{v}, \mathbf{v} \rangle_g^{-\frac{3}{2}} \cdot \langle \nabla_{\mathbf{v}}^g \mathbf{v}, \mathbf{v} \rangle_g \\ &= 0\end{aligned}$$

$$\begin{aligned}\frac{\nabla_{\mathbf{v}}^g \mathbf{v}}{\|\mathbf{v}\|_g} &= \mathbf{v} \cdot \langle \mathbf{v}, \mathbf{v} \rangle_g^{-\frac{3}{2}} \cdot \langle \nabla_{\mathbf{v}}^g \mathbf{v}, \mathbf{v} \rangle_g \\ \nabla_{\mathbf{v}}^g \mathbf{v} &= \mathbf{v} \cdot \langle \mathbf{v}, \mathbf{v} \rangle_g^{-1} \cdot \langle \nabla_{\mathbf{v}}^g \mathbf{v}, \mathbf{v} \rangle_g \\ \nabla_{\mathbf{v}}^g \mathbf{v} &= \frac{\langle \nabla_{\mathbf{v}}^g \mathbf{v}, \mathbf{v} \rangle_g}{\|\mathbf{v}\|_g^2} \cdot \mathbf{v} \\ &\quad \downarrow \\ &\quad \sigma\end{aligned}$$